3D inversion of AirMt AFMAG data

Alexander V. Gribenko, Michael S. Zhdanov, TechnoImaging and the University of Utah, Jean Legault, Shengkai Zhao, Geotech, Leif H. Cox, Glenn A. Wilson, TechnoImaging, and Keith Fisk, Geotech Airborne*

Summary

The Airborne Magnetic Tensor (AirMt) system measures the rotational invariants of the transfer functions for audio-frequency natural sources from helicopter platforms. AirMt, data are typically measured from 30 Hz to 720 Hz, giving detection depths down to 1 km or more, depending on the terrain conductivity. Given the airborne deployment, it is possible to acquire AirMt data over large areas for a relatively low cost compared to equivalent ground surveys. This makes it a practical method for mapping large-scale geological structures. We describe the theory of the AirMt system, and present a case study comparing 3D inversion results from ZTEM and AirMt surveys flown over the Nebo-Babel Ni-Cu-PGE deposit in Western Australia. Our 3D inversion results are shown to be in good agreement with the known geology of the deposits and the surrounding area.

Introduction

It has long been recognized that magnetovariational (MV) data can provide information about the deep 3D conductivity distribution in the earth (e.g., Berdichevsky and Zhdanov, 1984). The MV data can be expressed as the linear transfer functions (also known as magnetic tipper) relating the naturally occurring vertical to the horizontal magnetic field components. The basic reasoning is that the vertical magnetic field is zero for plane waves vertically propagating into a 1D (one-dimensional) earth. Nonzero vertical magnetic fields are thus directly related to 2D or 3D structures. This served as the basis for the development of the Z-axis Tipper Electromagnetic (ZTEM) system by Geotech. The ZTEM system measures the tipper components as the coefficients of a linear relationship between the vertical magnetic field measured from an airborne receiver to the horizontal components measured at a ground-based (reference) location. Similar to the impedance in magnetotelluric (MT) data, the calculation of the magnetic tipper effectively removes otherwise unknown source terms. In the framework of the ZTEM method, the receiver is flown via helicopter, meaning data can be rapidly acquired over large survey areas for relatively low cost compared to equivalent ground surveys. The time series of the magnetic fields are recorded at fixed sampling rates, and the data are binned and processed to generate in-phase and quadrature transfer functions (i.e., tippers) in the frequency domain as per Labson et al. (1985). The lowest frequency of the tipper depends on the speed of the helicopter, and the highest frequency depends on the sampling rate.

Another airborne MT method, AirMt, has been developed recently, (Kaminski et al., 2010; Kuzmin et al., 2010), which is effectively a generalized ZTEM system in that it directly measures the rotational invariant of the transfer functions for the three magnetic fields measured from an airborne receiver (Figure 1) to the three magnetic fields measured at a ground-based (reference) location (Figure 2). The lowest frequency of the transfer function depends on the speed of the airborne platform, and the highest frequency depends on the sampling rate. Transfer functions are typically obtained at five or six frequencies from 30 Hz to 720 Hz, giving skin depths ranging between 600 m and 2000 m for terrain conductivities typically encountered in ZTEM and AirMt surveys.

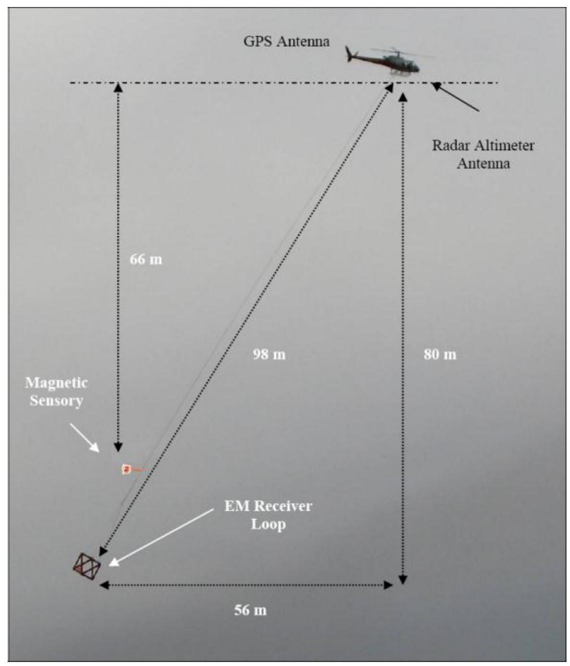

Figure 1. *AirMt AFMAG system deployed from a helicopter platform.*

In this paper, we introduce 3D inversion of AirMt data analogous to 3D MT inversion of Zhdanov et al. (2011). We present a case study from the Nebo-Babel Ni-Cu-PGE deposit in Western Australia that provides a direct comparison to 3D inversion of ZTEM data over the same area where both ZTEM and AirMt surveys were flown. Results are also compared with the 3D inversion of a GEOTEM time-domain AEM survey over the same area.

DOI http://dx.doi.org/10.1190/segam2012-1261.1

Figure 2. *A second set of AirMt coils are used for the reference station.*

3D modeling of AirMt data

For 2D and 3D geoelectrical structures, the magnetic field of a plane wave source will have a significant vertical component. Based on linear relationships between the different magnetic field components, it can be shown that:

$$H_z = W_{zx}H_x + W_{zy}H_y, \tag{1}$$

and this is called the *Weiss-Parkinson relationship* (Berdichevsky and Zhdanov, 1984). It reflects the fact that the vertical component of the magnetic field at every point is linearly related to the horizontal components of the same field. The values W_{zx} and W_{zy} form a complex vector, named the *Weiss-Parkinson Vector*, or the *induction vector*, or the *tipper*. The tipper, in contrast to the measured magnetic field, contains information about the 3D structure of the earth independent of the magnetic field's source. For ZTEM, the time series of the magnetic fields are recorded at fixed sampling rates, and the data are binned and processed to generate in-phase and quadrature transfer functions in the frequency domain as per Labson et al. (1985).

Assuming that the vertical magnetic field at the reference station is approximately zero, we can generalize the Weiss-Parkinson relationship such that the three components of a magnetic field measured at a receiver are linearly related to the horizontal magnetic fields measured at a ground-based (reference, R) location:

$$\begin{bmatrix} H_x \\ H_y \\ H_z \end{bmatrix} = \begin{bmatrix} W_{xx} & W_{xy} \\ W_{yx} & W_{yy} \\ W_{zx} & W_{zy} \end{bmatrix} \begin{bmatrix} H_x^R \\ H_y^R \end{bmatrix}. \tag{2}$$

If we write $\mathbf{W}_1$ and $\mathbf{W}_2$ as the first and second columns of the transfer functions, then we can introduce the variable:

$$\mathbf{K} = \mathbf{W}_1 \times \mathbf{W}_2, \tag{3}$$

and obtain the complex scalar:

$$K = \mathbf{K} \cdot Re(\mathbf{K})/|Re(\mathbf{K})|, \tag{4}$$

called the amplification parameter (AP), which can be shown to be rotationally invariant. This has certain advantages during acquisition, namely that the receiver orientation is irrelevant. For AirMt, the three components of the magnetic fields are recorded at both the airborne receiver and the reference station at fixed sampling rates, and the data are binned and processed to generate in-phase and quadrature transfer functions in the frequency domain (Kuzmin et al., 2010; Dodds, 2010, pers. comms.)

3D inversion methodology

Our 3D AirMt inversions are based on the re-weighted regularized conjugate gradient (RRCG) method, which updates the model conductivities, $\boldsymbol{\sigma}$, with an iterative scheme akin to:

$$\boldsymbol{\sigma}_{i+1} = \boldsymbol{\sigma}_i + \Delta\boldsymbol{\sigma}_i = \boldsymbol{\sigma}_i + k_i \mathbf{F}_i^{\mathrm{T}} \mathbf{r}_i,$$

where k_i is a step length, $\mathbf{F}_i^{\mathrm{T}}$ is the transpose of the $N_d \times N_m$ Fréchet matrix $\mathbf{F}_i$ of the normalized sensitivities, and $\mathbf{r}_i$ is the N_d length vector of the residual fields between the observed and predicted data. Traditional regularized inversion methods recover smooth solutions, and thus have difficulties recovering sharp boundaries between different geological formations without having a priori information about those boundaries enforced. Focusing regularization makes it possible to recover subsurface models with sharper resistivity contrasts and boundaries than can be obtained with smooth stabilizers, and do not require those boundaries to be enforced a priori (Zhdanov, 2002, 2009).

Our 3D frequency-domain modeling of magnetic fields and their sensitivities is based on an implementation of the contraction integral equation method that exploits the Toeplitz structure of large, dense matrix systems in order to solve multiple source vectors on the right-hand side using an iterative method with fast matrix-vector multiplications provided by a 2D FFT convolution (Hursán and Zhdanov, 2002). This implementation reduces storage and complexity, and lends itself well to large-scale parallelization. Once the Green's tensors have been precomputed, they are stored and re-used, further reducing run time. Once computed, the magnetic fields and their sensitivities can be transformed to the amplitude parameter. Given space limitations, specific details regarding these transforms are not included here.

DOI http://dx.doi.org/10.1190/segam2012-1261.1

Model study

We consider a model that consists of a 1 Ωm conductive L-shaped target embedded in a 100 Ωm host. The depth to the top of the target is 600 m and the thickness of the body is 400 m. The receivers were located in a 5 km x 5 km grid, separated by 200 m for a total of 676 receiver positions with flight elevation 75 m above the surface. The reference receiver was placed on the surface about 7 km away from the modeling domain. Synthetic data was computed at the standard set of AirMT frequencies: 30, 45, 90, 180, and 360 Hz. No noise were added to the data (Figure 3a,b).

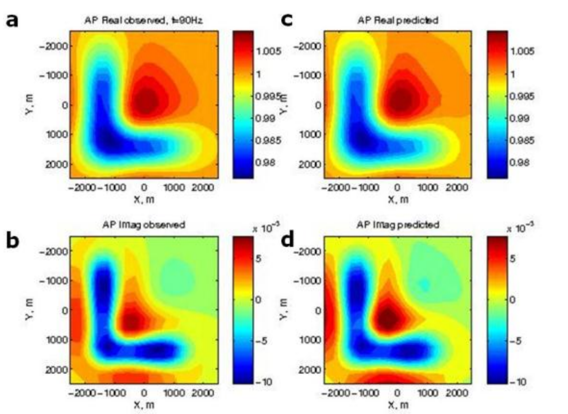

Figure 3. *Observed (left panels) and predicted (right panels) real (top panels) and imaginary (lower panels) amplitude parameter data.*

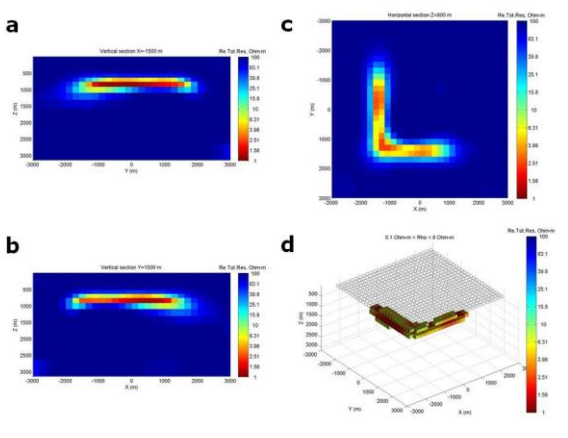

Figure 4. *3D AirMt inversion for the synthetic model: (a) Vertical cross section at x = -1500 m. (b) Vertical cross section at y = 1500 m. (c) Horizontal cross section at z = 800 m. (d) 3D perspective view of the L-shaped target with receiver positions shown by circles.*

Case study – Nebo-Babel, Western Australia

The Nebo-Babel Ni-Cu-PGE deposit in West Musgrave, Western Australia, is a world-class resource with drill intersections including 106.5 m at 2.4% Ni, 2.7% Cu, and 0.2g/t PGE; and a resource of about 1 million tonnes contained Ni and 1 million tonnes contained Cu+Co has been released. Babel is a large, low-grade disseminated deposit that subcrops through thin sand cover. Nebo, 2 km to the northeast, is buried under a few meters of aeolian dune sand and is smaller than Babel, but contains a number of high grade massive sulfide pods. The deposits were originally discovered using deflation lag sampling on a 1 km x 0.5 km grid. However, strong magnetic, electromagnetic, and gravity anomalies highlight the massive and disseminated mineralization, which is hosted within a shallowly WSW-plunging pipe of gabbronorite intrusive (1078Ma) offset by a fault (Figures 5 and 6). The Nebo-Babel deposit has a number of features in common with other Ni-Cu-PGE deposits hosted in dynamic magma conduits (e.g., Voisey's Bay, Canada), such as multiple magma pulses and sulfide entrainment from depth, rather than in situ sulfide segregation (Seat et al., 2007, 2009).

Under agreement between Geotech and BHP Billiton, both ZTEM and AirMt surveys were flown over the Nebo-Babel deposits. A total of 541 line km of ZTEM data and 574 line km of AirMt data were acquired along both east-west and north-south flight lines. These surveys are in addition to a previous GEOTEM survey flown over the deposits. The survey area has minimal topographic relief, varying from 460 to 494 m above sea level. The ZTEM receiver was flown with a nominal ground clearance of 78 m. ZTEM data were acquired at six frequencies; 25 Hz, 37 Hz, 75 Hz, 150 Hz, 300 Hz, and 600 Hz. The AirMt receiver was flown with a nominal ground clearance of 78 m. AirMt data were acquired at six frequencies; 24 Hz, 38 Hz, 75 Hz, 150 Hz, 300 Hz, and 600 Hz.

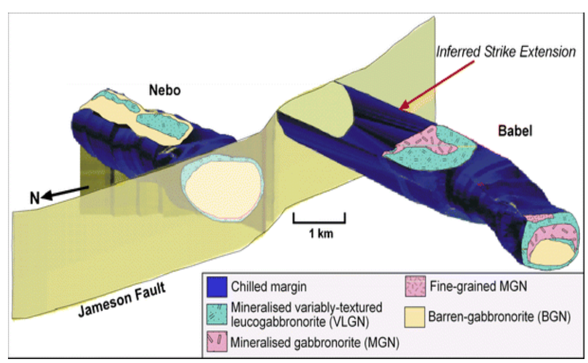

Figure 5. *3D geological model of the Nebo-Babel Ni-Cu-PGE deposit (from Seat et al., 2007).*

DOI http://dx.doi.org/10.1190/segam2012-1261.1

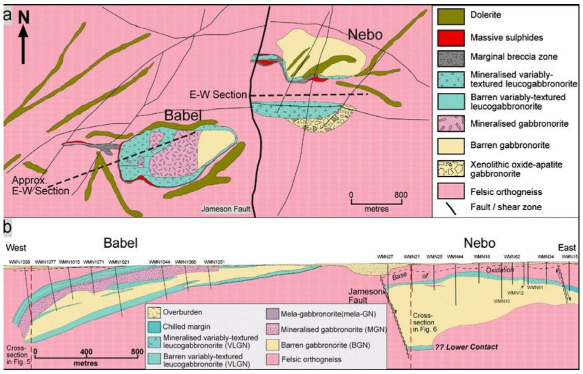

Figure 6. *Geology of the Nebo and Babel deposits (from Seat et al., 2007).*

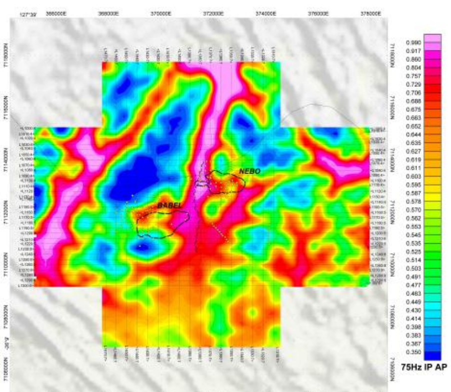

Figure 7. *75 Hz inphase amplitude parameter data.*

For both ZTEM and AirMt inversions, the earth model was discretized into 322,560 cells of 75 m x 75 m horizontal dimension that varied from 8 m thickness near the surface to 126 m thickness at 2 km depth. Both inversions began from a 300 Ωm homogeneous half-space. The Jameson Fault is a dominant feature in both the ZTEM and AirMt data (e.g., Figure 7). Horizontal and vertical cross sections from models obtained from 3D inversion of the AirMt data are shown in Figures 8 and 9, respectively. While not shown (for space limitations), both ZTEM and AirMt inversions recovered similar structures. Note that both the Nebo and Babel deposits are recovered as structures that appear to offshoot the Jameson Fault.

Conclusions

AirMt represents a practical airborne method for mapping conductivity contrasts to depths in excess of 1 km. Interpretation of AirMt data is analogous to ZTEM data, and is similar in principle to MT data inversion. We have developed a 3D inversion methodology for AirMt data based on the regularized re-weighted conjugate gradient (RRCG) method with focusing stabilizers. 3D modeling is based on our implementation of the integral equation method. The software is fully parallelized, meaning that it can be scaled to very large survey areas. We have demonstrated this with the 3D inversion of ~500 line km of AirMt data from the Nebo-Babel Ni-Cu-PGE deposit in Western Australia's West Musgrave district. Both inversions recovered structures related to the Nebo and Babel deposits. At the time of writing, comparison of the ZTEM and AirMt models to those obtained by 3D inversion of GEOTEM time-domain AEM data (Cox et al., 2010) had not been completed.

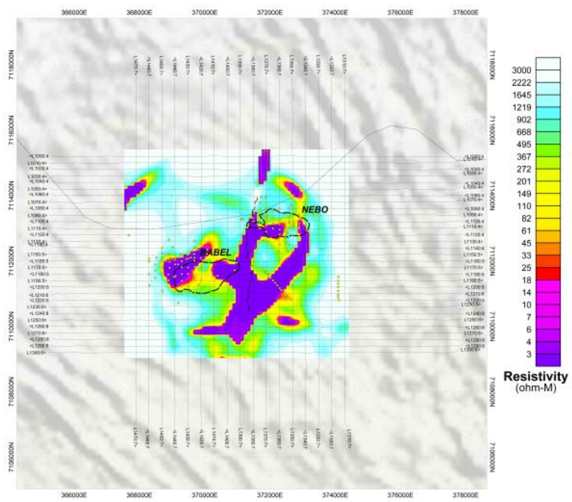

Figure 8. *Horizontal cross section of the resistivity as recovered from 3D inversion of the AirMt data.*

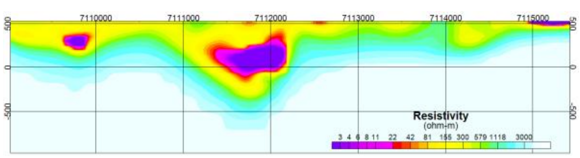

Figure 9. *Vertical cross section along the NS-oriented line L1430 of the resistivity as recovered from the 3D inversion of the AirMt data. This line transects the Babel deposit, as is clearly visible.*

Acknowledgements

The authors acknowledge TechnoImaging, Geotech, Geotech Airborne, and BHP Billiton for permission to publish. Gribenko and Zhdanov acknowledge support of the University of Utah's Consortium for Electromagnetic Modeling and Inversion (CEMI).

DOI http://dx.doi.org/10.1190/segam2012-1261.1

http://dx.doi.org/10.1190/segam2012-1261.1

EDITED REFERENCES

Note: This reference list is a copy-edited version of the reference list submitted by the author. Reference lists for the 2012 SEG Technical Program Expanded Abstracts have been copy edited so that references provided with the online metadata for each paper will achieve a high degree of linking to cited sources that appear on the Web.

REFERENCES

Berdichevsky, M. N., and M. S. Zhdanov, 1984, Advanced theory of deep geomagnetic sounding: Elsevier.

Cox, L. H., G. A. Wilson, and M. S. Zhdanov, 2010, 3D inversion of airborne electromagnetic data using a moving footprint: Exploration Geophysics, **41**, 250–259.

Hursán, G., and M. S., Zhdanov, 2002, Contraction integral equation method in three-dimensional electromagnetic modeling: Radio Science, **37**, doi: 10.1029/2001RS002513.

Kaminski, V. F., P. Kuzmin, and J. M. Legault, 2010, AirMt — Passive airborne EM system: Presented at 3rd CMOS-CGU Congress.

Kuzmin, P. V., G. Borel, E. B. Morrison, and J. Dodds, 2010, Geophysical prospecting using rotationally invariant parameters of natural electromagnetic fields: WIPO International Patent Application No. PCT/CA2009/001865.

Labson, V. F., A. Becker, H. F. Morrison, and U. Conti, 1985, Geophysical exploration with audio frequency natural magnetic fields: Geophysics, **50**, 656–664.

Seat, Z., S. W. Beresford, B. A. Grguric, M. A. M. Gee, and N. V. Grassineau, 2009, Reevaluation of the role of external sulfur addition in the genesis of Ni-Cu-PGE deposits — Evidence from the Nebo-Babel Ni-Cu-PGE deposit, West Musgrave, Western Australia: Economic Geology, **104**, 521–538.

Seat, Z., S. W. Beresford, B. A. Grguric, R. S. Waugh, J. M. A. Hronsky, M. A. M. Gee, D. I. Groves, and C. I. Mathison, 2007, Architecture and emplacement of the Nebo-Babel gabbronorite-hosted magmatic Ni-Cu-PGE sulphide deposit, West Musgrave, Western Australia: Mineralium Deposita, **42**, 551–581.

Ward, S., 1959, AFMAG — Airborne and ground: Geophysics, **24**, 761–787.

Ward, S. H., J. O. Donnell, R. Rivera, G. H. Ware, and D. C. Fraser, 1966, AFMAG — Applications and limitations: Geophysics, **31**, 576–605.

Zhdanov, M. S., 2002, Geophysical inverse theory and regularization problems: Elsevier.

Zhdanov, M. S., 2009, Geophysical electromagnetic theory and methods: Elsevier.

Zhdanov, M. S., R. B. Smith, A. Gribenko, M. Cuma, and A. M. Green, 2011, Three-dimensional inversion of large-scale EarthScope magnetotelluric data based on the integral equation method — Geoelectrical imaging of the Yellowstone conductive mantle plume: Geophysical Research Letters, **38**, L08307, doi: 10.1029/2011GL046953.